Fluorescence Lifetime Spectroscopy in Multiply Scattering Media with Dyes Exhibiting Multiexponential Decay Kinetics

Eddy Kuwana and Eva M. Sevick-Muraca

Departments of Chemistry and Chemical Engineering, Texas A&M University, College Station, Texas 77843-3122 USA

ABSTRACT   To investigate fluorescence lifetime spectroscopy in tissue-like scattering, measurements of phase modulation as a function of modulation frequency were made using two fluorescent dyes exhibiting single exponential decay kinetics in a 2% intralipid solution. To experimentally simulate fluorescence multiexponential decay kinetics, we varied the concentration ratios of the two dyes, 3,3-diethylthiatricarbocyanine iodide and indocynanine green (ICG), which exhibit distinctly different lifetimes of 1.33 and 0.57 ns, respectively. The experimental results were then compared with values predicted using the optical diffusion equation incorporating 1) biexponential decay, 2) average of the biexponential decay, as well as 3) stretched exponential decay kinetic models to describe kinetics owing to independent and quenched relaxation of the two dyes. Our results show that while all kinetic models could describe phase-modulation data in nonscattering solution, when incorporated into the diffusion equation, the kinetic parameters failed to likewise predict phase-modulation data in scattering solutions. We attribute the results to the insensitivity of phase-modulation measurements in nonscattering solutions and the inaccuracy of the derived kinetic parameters. Our results suggest the high sensitivity of phase-modulation measurements in scattering solutions may provide greater opportunities for fluorescence lifetime spectroscopy.

INTRODUCTION

Fluorescence lifetime spectroscopy is especially advantageous for quantitative biomedical spectroscopy of analytes since the measurement of fluorescence decay kinetics (rather than the fluorescence intensity) eliminates the necessity for the knowledge of the analyte-sensing fluorophore concentration. Frequency domain techniques provide measurement of fluorescence lifetime (τ) using simple relationships of the phase-delay (θ) and amplitude-attenuation (M) of the reemitted fluorescence as a function of the modulation frequency relative to intensity modulated excitation light. However, the development of fluorescence lifetime spectroscopy for near infrared (NIR) biomedical tissue diagnostics for sensing using systematically administered dyes (Hawrysz and Sevick-Muraca, 2000; Weissleder et al., 1999) or implantable devices (Qing et al., 1997; Russell et al., 1999) requires 1) deconvolving the influence of multiple scatter upon the measured emission phase-delay and amplitude-attenuation measured in the NIR wavelength region and 2) accounting for nonsingle exponential decay kinetics.

Most fluorophores capable of analyte sensing exhibit multiexponential kinetics. For example, Ca^{2+} (Lakowicz and Szmacinski, 1992) and pH (Lakowicz and Szmacinski, 1993) sensing with fluorescence lifetime spectroscopy in dilute, nonscattering solutions requires determination of multiexponential decay kinetics for accurate analyte sensing. Accurate fluorescence lifetime spectroscopy in the presence of tissue-like scattering requires a model that ac-

counts not only for photon propagation but also for multiexponential decay kinetics as well. Indeed, the fluorescence resulting from ultraviolet excitation of the normal and athlerosclerotic arterial wall also shows multiexponential decay kinetics of its excitable constitutes (Andersson-Engels et al., 1991). Because ultraviolet light does not multiply scatter in tissues, deconvolution of the influence of scatter is not necessary. In contrast, failure to properly account for multiply scattered NIR excitation and emission light in tissue or within a scattering solution can result in erroneous identification of intrinsic decay kinetics. Upon conducting phase-modulation measurements on a solution of intralipid containing the NIR excitable fluorophore, indocyanine green (ICG), Lakowicz and Abugo (1999) did not incorporate the propagation of light, yet attribute multiexponential decay kinetics to this dye, which typically exhibits single exponential decay kinetics.

Approaches to appropriately model the multiple scattering of NIR excitation and fluorescence photons and to use diffusion models for quantitative spectroscopy have been previously demonstrated (Hutchinson et al., 1996; Cerussi et al., 1997; Mayer et al., 1999) for dyes exhibiting single exponential decay kinetics. Because most dyes exhibit multiexponential decay kinetics or exist within two or more different states, lifetime spectroscopy within tissues or other scattering media must consider kinetics beyond simple, first order decay. Indeed, the presence of scattering increases the sensitivity of frequency-domain measurements and accurate kinetic models need to be considered. However, to date, there has been no attempt to perform lifetime spectroscopy of dyes exhibiting multiexponential decays in tissue-like scattering media. Herein, we present a model-based, experimental study of fluorescence involving two dyes with distinctly different lifetimes combined together at various concentration ratios in a multiply scattering medium. By

---

varying the concentration ratios of short- and long-lived dyes, we tested the models and identify a feasible approach for quantitative characterization of multiexponential decay kinetics in tissues as well as in implantable sensors.

Because fluorescent decay kinetics may also reflect quenching, we also investigated incorporation of the stretched exponential decay kinetics into the diffusion equation to predict experimental measurements. The use of multi- and stretched exponential functions accounts for intrinsic kinetics of the fluorescence decay, whereas the diffusion equation accounts for the influence of excitation and emission light propagation through scattering media. Upon combining the fluorescence decay models with the diffusion equation describing light propagation, we seek to describe the propagation and generation of emission light from analyte-sensing fluorophores for quantitative spectroscopy on the basis of first principles.

In the following, we briefly provide background and theory for fluorescence decay kinetics, light propagation in scattering media, and fluorescent light generation and propagation in scattering media. We then describe the instrumentation and frequency-domain measurements of scattering and nonscattering solutions containing mixtures of two dyes (ICG and 3,3-diethylthiatricarbocyanine iodine (DTTCI)) exhibiting distinct single exponential decay times.

BACKGROUND AND THEORY

Multiexponential decay fluorescence measurement in nonscattering media

The impulse response function $I(t)$ for a multiexponential decay model, fitted to a sum of n exponentials, is described by (Lakowicz, 1983)

$$I(t)_{\mathrm{mult}} = \sum_{j=1}^{n} a_j e^{-t/\tau_j} \qquad (1)$$

in which a_j is a preexponential factor representing the fractional contribution to the time-resolved decay of the component with a lifetime τ_j. The average lifetime τ_{avg} for a fluorophore experiencing multiexponential decay kinetics is given by $\tau_{\mathrm{avg}} = \sum_j f_j \tau_j$ in which f_j represents the fractional steady-state intensity of each component in the mixture and can be calculated if a_j and τ_j are available (Lakowicz, 1983). The values of a_j and τ_j for a given sample can be estimated from frequency-domain measurements of phase-shift $\theta(\omega)$ and modulation-ratio $M(\omega)$ by minimizing the error-weighted sum of the squared deviations between the measured and predicted values (χ^2) (Gratton et al., 1984).

Stretched exponential decay function in nonscattering media

In many cases, decay profiles from complex systems can be fitted more appropriately by stretched exponential function of the form (Inokuti and Hirayama, 1965; James and Ware, 1985; Nemzek and Ware, 1975):

$$I(t)_{\mathrm{st-exp}} = a e^{(-\alpha t - \beta t^{0.5})} \qquad (2)$$

in which α and β are functions of diffusion coefficients of the fluorophore and quencher, their encounter distance, and the quencher concentration. The type of decay profile in Eq. 2 has also been studied to model diffusion controlled reactions as applied to a first-order (simplest case) fluorescence quenching kinetics (Nemzek and Ware, 1975). Herein we use the stretched exponential function to account for potential fluorescence quenching of one dye by another as well as between the two dyes whose fluorescence is collectively measured. In the former case the intrinsic decay kinetics from simultaneously emitting dyes is expressed as $I(t) = a_1 \exp(-t/\tau_1) + a_2 \exp(-\alpha t - \beta t^{0.5})$, and in the latter case, by $I(t) = a_1 \exp(-\alpha_1 t - \beta_1 t^{0.5}) + a_2 \exp(-\alpha_2 t - \beta_2 t^{0.5})$.

Hirayama et al. (1990) showed that the stretched exponential function in Eq. 2 could be approximated by the sum of n exponential terms.

$$f(t) = a e^{(-\alpha t - \beta t^{0.5})} \approx \sum_{j=1}^{n} a_j e^{-t/\tau_j} \qquad (3)$$

If a set of a_j and τ_j values are available from a sufficient number, n, of exponential terms, they can be used to generate a decay profile from which the parameters α and β can be extracted using the relationship given in Eq. 3 (Hirayama et al., 1990). In this investigation, we similarly extract stretch exponential decay parameters from the multiexponential decay model containing the optimal number of components, n, which fit the nonscattering data with the greatest degree of correlation.

Optical diffusion equation

Whereas the intrinsic decay kinetics provides the information for fluorescence lifetime spectroscopy, the kinetics must be used and derived within the context of the diffusion equation to appropriately account for the influence of multiple light scattering. The diffusion approximation to the radiative transfer equation describing the time-dependent transport of light through a highly scattering medium is given by

$$\frac{\partial U(r, t)}{\partial t} - vD\nabla^2 U(r, t) + v\mu_a U(r, t) = q_0(r, t) \qquad (4)$$

in which

$$D = \{3[\mu_a + \mu_s(1 - g)]\}^{-1} \qquad (5)$$

$U(r, t)$ is the density of photons at position r and time t; v is the speed of light within the medium; D is the optical diffusion coefficient; μ_a is the linear absorption coefficient (i.e., the inverse of the mean free path for photon absorption

with units of inverse distance); μ_s is the linear scattering coefficient (i.e., the inverse of the mean free path for photon scattering); g is the average of the cosine of the scattering angle; and $q_0(r, t)$ is the photon source. The term $\mu_s(1 - g)$ is often referred as the isotropic scattering coefficient μ_s'.

Eq. 4 has been solved for an infinite medium to yield an equation describing transport of light through a scattering medium (e.g., tissue) for the case of a sinusoidally modulated point source of light (frequency-domain) (Fishkin and Gratton, 1993). The development of time- and frequency-domain photon migration technique for characterization of tissue absorbance and scattering has been well established (Sevick et al., 1991).

Generation of fluorescence light from a dye exhibiting single, multi-, and stretched exponential decay

The photon density of fluorescent light, U_f, which is generated and propagates within the multiple scattering medium, can also be described by Eq. 4, provided that its source emission kinetics is properly modeled. When a fluorophore is distributed uniformly in a random media, the photon density of excitation light, U_x, experiences absorption owing to the fluorophore, in which μ_{afx} is the absorption coefficient proportional to the fluorophore concentration. The radiative relaxation of the activated fluorophore serves at a distributed source of emission light within the random media. The assumptions are: 1) the fluorophore concentrations are dilute so that the probability that a fluorophore will absorb emission light and refluoresce (i.e., secondary fluorescence) is negligible; and 2) photobleaching does not occur. The emission source q_m in frequency domain for single, multi-, and stretched exponential decay kinetics are:

$$q_m(r, \omega) = v\mu_{afx}\left(\frac{1}{1 - i\omega\tau}\right)U_s(r, \omega)_{ac}\phi\Xi_m \quad (6)$$

$$q_m(r, \omega)_{mult} = \mu_{afx}\int_0^\infty (I(t)_{mult}e^{(i\omega t)}dt)U_x(r, \omega)_{ac}\phi\Xi_m$$

$$= v\mu_{afx}\left(\sum_j \frac{a_j}{1 - i\omega\tau_j}\right)U_x(r, \omega)_{ac}\phi\Xi_m \quad (7)$$

$$q_m(r, \omega)_{st-exp} = v\mu_{afx}\int_0^\infty (I(t)_{st-exp}e^{(i\omega t)}dt)U_x(r, \omega)_{ac}\phi\Xi_m$$

$$(8)$$

in which $U_x(r, \omega)$, ϕ, and Ξ_m are excitation photon density, quantum efficiency of the fluorophore, and the detection efficiency factor of the system at the emission wavelength (which contains the system spectral response and the flu-

orophore spectral emission efficiency (Lakowicz and Szmacinski, 1993)). The sources of emission light from a mixture of fluorophores undergoing single-, multiple-, or stretched exponential decays are simply a combination of the above expressions.

Upon using Eqs. 6 to 8 as the source term in Eq. 4, the generated fluorescence photon-density U_f can then be solved for single, multi-, and stretched exponential decay kinetics:

$$U_f(r, \omega)_{ac} = \frac{\mu_{afx}\phi\Xi_m(SA)}{4\pi vD_xD_mr} \frac{1}{[1 + (\omega\tau)^2]}$$
$$\times \{[\psi - \kappa\omega\tau] + i[\kappa + \psi\omega\tau]\} \quad (9)$$

$U_f(r, \omega)_{ac,mult}$

$$= \frac{\mu_{afx}\phi\Xi_m(SA)}{4\pi vD_xD_mr}\left\{(\psi - i\kappa)\left(\sum_j \frac{a_j}{1 - i\omega\tau_j}\right)\right\}$$

$$= \frac{\mu_{afx}\phi\Xi_m(SA)}{4\pi vD_xD_mr}\left\{\left[\psi\sum_j \frac{a_j}{1 + \omega^2\tau_j^2} - \kappa\sum_j \frac{a_j\omega\tau_j}{1 + \omega^2\tau_j^2}\right]\right.$$

$$\left. + i\left[\kappa\sum_j \frac{a_j}{1 + \omega^2\tau_j^2} + \psi\sum_j \frac{a_j\omega\tau_j}{1 + \omega^2\tau_j^2}\right]\right\} \quad (10)$$

$$U_f(r, \omega)_{ac,st-exp} = \frac{\mu_{afx}\phi\Xi_m(SA)}{4\pi vD_xD_mr}$$

$$\times \left\{(\psi - i\kappa)\int_0^\infty (I(t)_{st-exp}e^{(i\omega t)}dt)\right\}$$

$$(11)$$

in which S is the fluence of the source (photons per second); A is the modulation of the source; i is a complex number ($i = \sqrt{-1}$); ω is the angular modulation frequency of the source; D_x and D_m are the diffusion coefficients at excitation and emission wavelengths, respectively. The terms ψ and κ are functions of optical properties (μ_a and μ_s), v, and ω. In the case of multiexponential decay kinetics, an additional fluorescence photon density equation can be derived by incorporating the τ_{avg}, which results in an equation similar to that of Eq. 9.

$$U_f(r, \omega)_{ac,mult-avg} = \frac{u_{afx}\phi\Xi_m(SA)}{4\pi vD_xD_mr} \frac{1}{[1 + (\omega\tau_{avg})^2]}$$
$$\times \{[\psi - \kappa\omega\tau_{avg}] + i[\kappa + \psi\omega\tau_{avg}]\} \quad (12)$$

For the mixture of two fluorophores of which one is quenched by the other, the measured fluorescence should be predicted by a combination of Eqs. 9 and 11.

The photon density can be related to the experimentally measured phase-shift (θ) and modulation-ratio (M) as a
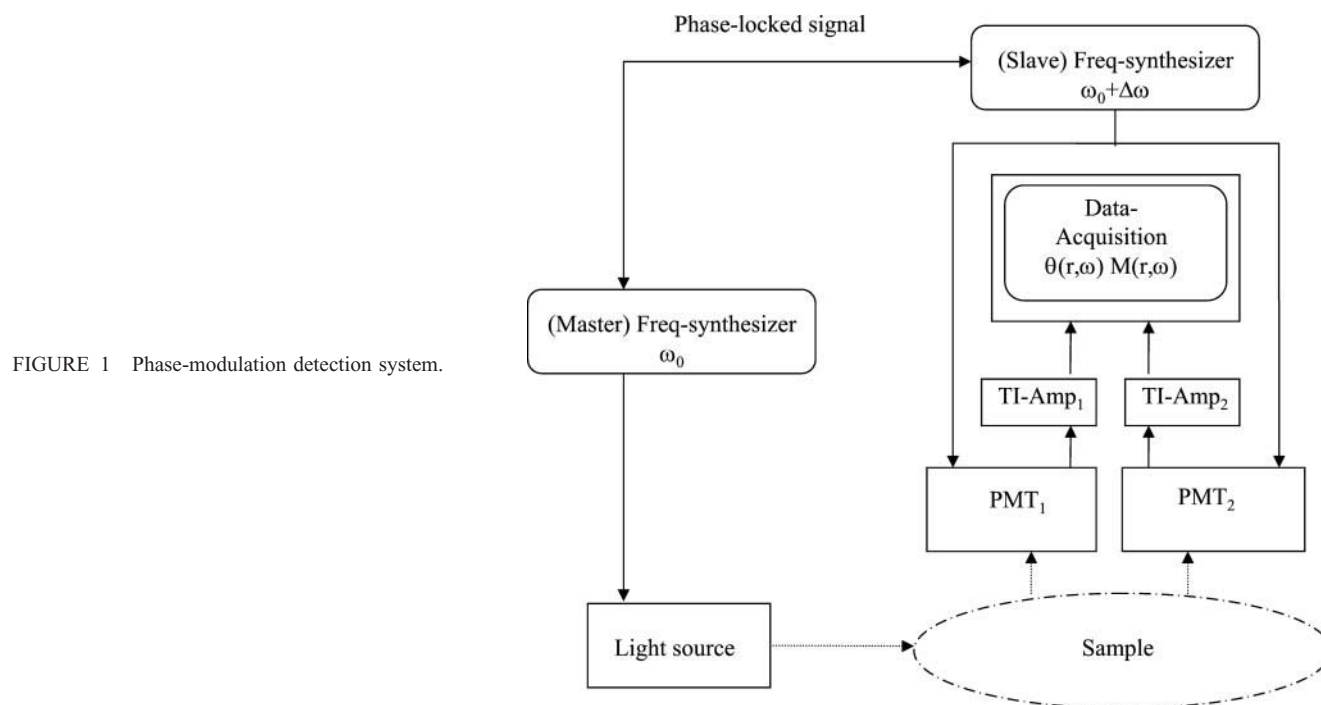
Phase-locked signal

FIGURE 1   Phase-modulation detection system.

function of modulation frequency (Lakowicz et al., 1984). The relationship between fluorescence photon density to the measured fluorescence phase-shift θ_f and modulation-ratio M_f for a dye undergoing single exponential decay kinetics in multiply scattering solutions has been obtained (Mayer et al., 1999). The measured fluorescence phase-shift θ_f and modulation-ratio M_f for a dye exhibiting multiexponential decay kinetics can also be obtained using similar relationship. In the case in which the decay kinetics are described by stretched exponential decay kinetics, numerical integration needs to be performed in solving the integration in Eq. 11 prior to attaining a useful relationship between the fluorescence photon density to the measurable quantities.

MATERIALS AND METHODS

Dyes and solutions

Two fluorescence dyes with distinct lifetimes, ICG (Aldrich Inc., Milwaukee, WI) and DTTCI (Acros Organics—Fisher Scientific, Fair Lawn, NJ) were chosen in this study because they can both be excited at 780 nm, and their emission at 830 nm can be observed simultaneously, giving rise to apparent multiexponential decay kinetics if relaxation of the dyes occur independently. If quenching of at least one of the two dyes occurs, stretched exponential decay kinetics should be evident. The dyes were dissolved in a mixture (1:1 volumetric ratio) of water and ethanol (EtOH, A406 P, Fisher Scientific, Fair Lawn, NJ) and added to aqueous intralipid solution (Abbott Laboratories, North Chicago, IL) to mimic the scattering properties of biological tissue.

Instrumentation and data acquisition

The data acquisition system schematic used for frequency domain photon migration (FDPM) measurements is illustrated in Fig. 1 and briefly dis-

cussed in the following. Two photomultiplier tubes (PMT) (Model H6573, Hamamatsu, Tokyo Japan) were gain modulated by an amplified (ENI Amplifier, Model 403 LA, Rochester, NY) radiofrequency (RF) signal from a frequency synthesizer (Marconi Instruments Signal Generator 2022A, Mountain View, CA), that was phase-locked to a second master oscillator used for laser diode source modulation. The detectors were outfitted with neutral-density filters (CVI Laser, Albuquerque, NM), narrow-bandpass interference filters (10 nm full width half maximum, CVI Laser), and focusing lens assemblies. In addition to neutral-density filters at the photocathode, a neutral-density filter wheel was also used in the setup to aid in adjusting DC levels of the detected PMT signals. The PMTs were modulated at the same frequency as the source (ω_0, on the order of 10 to 100 MHz), plus a small offset frequency ($\Delta\omega$, 100 Hz). The result of mixing at the detector (i.e., heterodyning) was a sinusoidal signal, which contained frequencies of $\Delta\omega$ as well as higher frequencies. These higher frequencies were removed by transimpedance-amplifiers (TI-Amp, Model 70710, Oriel, Stratford, CT), which acted as low pass filters, and are shown in Fig. 1 as TI-Amp. Consequently, the mixed signal, after passing through TI-Amp, was collected via standard data acquisition software (Labview 5.0, National Instruments, Austin, TX) and was processed to extract phase and modulation information. Depending upon the measurement (see below), the source was either a 828-nm diode (40 mW, Thorlabs Inc., Newton, NJ) or a 778-nm diode (25 mW, DFS series; Melles Griot, Boulder, CO) that was modulated by the master oscillator.

Measurement of fluorescence lifetime in nonscattering solution

Fig. 2 *A* illustrates the incident and detected light schemes typical of fluorescence measurements in nonscattering solutions (Lakowicz, 1983). The incident excitation light is directed to a beam splitter, which directed approximately approximately one-third of the light to PMT_1 via 1000-μm optical fiber (HCP-M1000T-08, Spectran, Avon, CT), whereas the remaining portion was delivered to the sample. A second fiber collected the fluorescent signal generated within the sample and directed the signal to PMT_2. A 780-nm interference filter was used at PMT_1 and an 830-nm
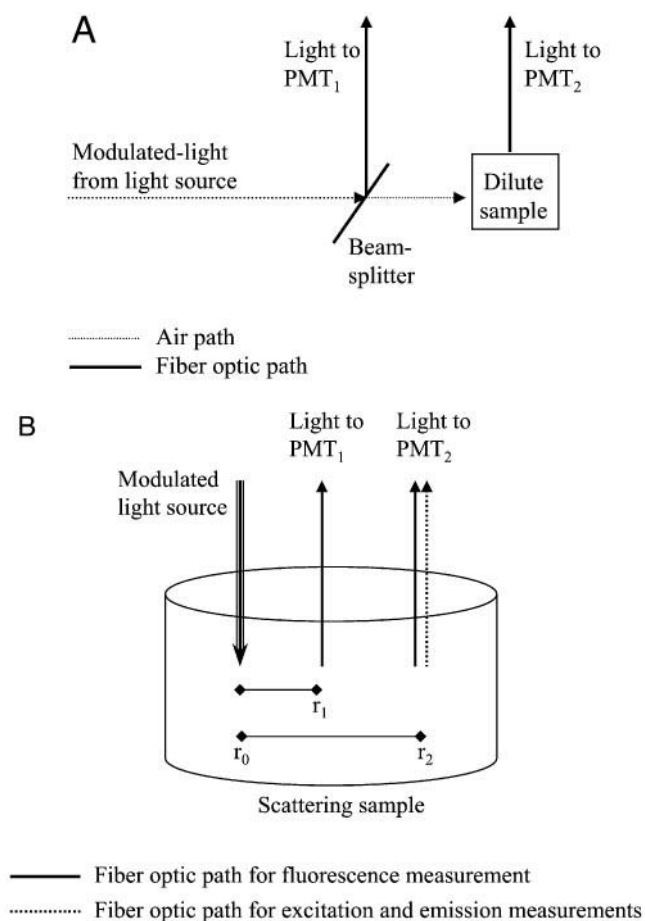
FIGURE 2 (*A*) Source and fiber-optically coupled detection schematic for fluorescence measurements in dilute, nonscattering solutions. (*B*) Fiber-optically coupled source and detectors placement for fluorescence, excitation, and emission measurements in scattering media. Fluorescence measurements used 778-nm source, a 780-nm interference filter at PMT_1, and an 830-nm interference filter at PMT_2 to collect fluorescent light. When multiplexing was performed, the interference filters were switched as well. Excitation measurements used 778-nm source and 780-nm interference filters at both PMTs. Emission measurements used 828-nm source and 830-nm interference filters at both PMTs.

interference filter was used at PMT_2. The phase-shift and modulation-ratio measured at PMT_2 for each sample were taken as a function of modulation frequency (10–120 MHz), and reported relative to that measured at PMT_1. As described in Appendix A, lifetime determination from phase-shift and modulation-ratio measurements in nonscattering media required a reference measurement.

Measurement of fluorescence lifetime in scattering solution

The incident and detected light configurations for measurements in scattering solutions are depicted in Fig. 2 *B*. Three different measurements were performed on fluorescent scattering samples, 1) the fluorescence measurement, 2) the excitation measurement, and 3) the emission measurement. The fluorescence measurement of phase-shift and modulation-ratio (θ_f and M_f) includes photon migration at the excitation wavelength, generation of fluorescence, propagation at the emission wavelength, as

well as the fluorescence decay kinetics. The excitation measurement of phase-shift and modulation ratio (θ_x and M_x) and emission measurement of (θ_m and M_m) are due solely to photon migration at excitation and emission wavelengths.

For the case of fluorescence measurements in scattering solutions, an optical fiber carrying the incident light (778 nm) was submerged inside the sample so the solution to the diffusion equation for infinite media was not violated. A second fiber, at a distance r_1 from the source fiber, collected the attenuated optical signal and directed the signal to PMT_1. At a distance r_2 from the source fiber, a third optical fiber collected the further attenuated signal and directed it to PMT_2. Measurement was conducted with a 780-nm interference filter at the PMT that enabled measurement of the attenuated optical signal at the excitation wavelength and an 830-nm interference filter at the one that measured the signal at fluorescence wavelength. The phase-shift and modulation-ratio data for each sample was taken at a range of modulation frequencies (10–120 MHz).

The sample systems for excitation measurement and emission measurement in scattering solutions were similar. The only difference was the wavelength of the light source. Whereas light of 778 nm was used for excitation measurement, 828 nm light source was used for emission measurement. Interference filters were used in both PMTs to select 780-nm light for excitation measurements and 830-nm light for emission measurements. For both measurement cases (excitation and emission), the light was directed to a beam splitter (not shown). The smaller portion of the light was directed to PMT_1 via optical fiber (not shown), whereas the remaining portion was delivered into the sample. A second fiber, at varying distance ($r_2 - r_o$), collected the attenuated optical signal from inside the sample and directed the signal to PMT_2. Excitation and emission measurements were conducted to provide optical property measurements at the two wavelengths.

The data acquired consisted of AC intensity (I_{ac}) and DC intensity (I_{dc}) measured at both PMTs, as well as the relative phase (θ_{rel}) between the two PMTs, as a function of modulation frequency. For each measurement at a given modulation frequency, 20,480 of data sets (each set consists of one value I_{ac}, I_{dc}, and θ_{rel}) in a total of 10 cycles that were collected in approximately 2 s. The DC intensity was determined from the average AC-intensity value of collected signals. The value of the DC intensity was then subtracted from each detected value, and a fast Fourier transform analysis was performed to provide AC and θ.

Multiplexing and calibration

The phase and amplitude of the detected signal is subject to the detection system's response functions. The effective response functions (i.e., θ_{instr} and M_{instr}), which are defined as the combined response function effects of the two measurement channels, are mainly due to differences in timing characteristics of the PMTs, TI-Amps, and analog data cables. The differences in timing characteristics of the two measurement channels may corrupt the phase and modulation (i.e., I_{ac}/I_{dc}) information during the signal processing. Therefore, it is important that corrections that are outlined in the Appendices A and B for these response function effects to be performed.

RESULTS AND DISCUSSIONS

The sample identification and compositions used in the experimental study are summarized in Table I. The excitation and emission spectra of 0.4 μM ICG and 0.5 μM DTTCI in 50% (volume) EtOH are shown in Fig. 3. The spectra were obtained by SPEX FLUOROLOG-2 (Model F212I, Jobin Yvon Spex, Edison, NJ) and recorded by SPEX DM3000F. In the case of scanning the excitation spectrum, the emission wavelength was stationed at 780 nm,

TABLE 1 Summary of sample compositions

Sample name	ICG (μM)	DTTCI (μM)	Solvent
DTTCI-dilute		0.5	EtOH/H_2O
ICG-dilute	0.4		EtOH/H_2O
SAMPLE A	0.05	0.5	EtOH/H_2O
SAMPLE B	0.15	0.5	EtOH/H_2O
SAMPLE C	0.4	0.5	EtOH/H_2O
DTTCI-scatter		0.5	2% Intralipid in EtOH/H_2O
ICG-scatter	0.4		2% Intralipid in EtOH/H_2O
SAMPLE D	0.05	0.5	2% Intralipid in EtOH/H_2O
SAMPLE E	0.15	0.5	2% Intralipid in EtOH/H_2O
SAMPLE F	0.4	0.5	2% Intralipid in EtOH/H_2O

whereas in the case of emission spectrum scanning, the excitation wavelength was stationed at 830 nm.

## Fluorescence multi- and stretched exponential decay in nonscattering media

Measurements in nonscattering solutions was performed at various ICG-DTTCI concentration ratios; SAMPLE A (0.05 μM ICG and 0.5 μM DTTCI), SAMPLE B (0.15 μM ICG and 0.5 μM DTTCI), and SAMPLE C (0.4 μM ICG and 0.5 μM DTTCI). Each sample was diluted in 50% (volume) EtOH. The dye concentrations were determined to obtain adequate signal strength and resolution at various ICG-DTTCI concentration ratios.

The sample used as the reference was 0.5 μM of DTTCI in EtOH and provided measurements of θ_{rel}^{ref} and M_{rel}^{ref} as

outlined in Appendix A. The lifetime of DTTCI in EtOH is known to be 1.33 ns (Mayer et al., 1999). The measurement data of phase-shift θ_{rel} and modulation ratio M_{rel} are substituted into Eqs. A5 and A6 (see Appendix A), and the values of θ and M after correction for the instrument function are plotted in Fig. 4. The phase-shift and modulation-ratio data at each concentration ratio was used to obtain the parameters a_j and τ_j at the minimum value of χ^2 using the Nelder-Mead method (Matlab Optimization Toolbox) (Press et al., 1992). The frequency domain data were analyzed for a_j and τ_j in terms of a biexponential model as well as an average lifetime model—both correspond to independent radiative relaxation of the two dyes. The results are listed in Table 2a. The fractional steady-state parameter of species 1 (f_1) increases with ICG concentration as one would expect for independent relaxation of the two dyes.

The lifetimes τ_1 and τ_2 are expected to be constant at different concentration ratios, if negligible quenching between ICG and DTTCI occurs. The variation of τ_1 and τ_2 with concentration ratio may be due to the error associated with the optimization. An optimization study was also performed using synthetic data generated with some randomly distributed error model (data not shown for brevity). The study shows that χ^2 optimization of synthetic phase-shift and modulation-ratio data with 1% random error in the phase-modulation data within the frequency range as high as 120 MHz resulted in as much as 50% and 5% deviations from the true values for lifetime for ICG and DTTCI. For similar synthetic phase-modulation data at modulation frequency as high as 350 MHz, the deviations

FIGURE 3 Excitation (emission at 830 nm) and emission (excitation at 780 nm) spectra of 0.4 μM ICG and 0.5 μM DTCCI solution in 50% EtOH.
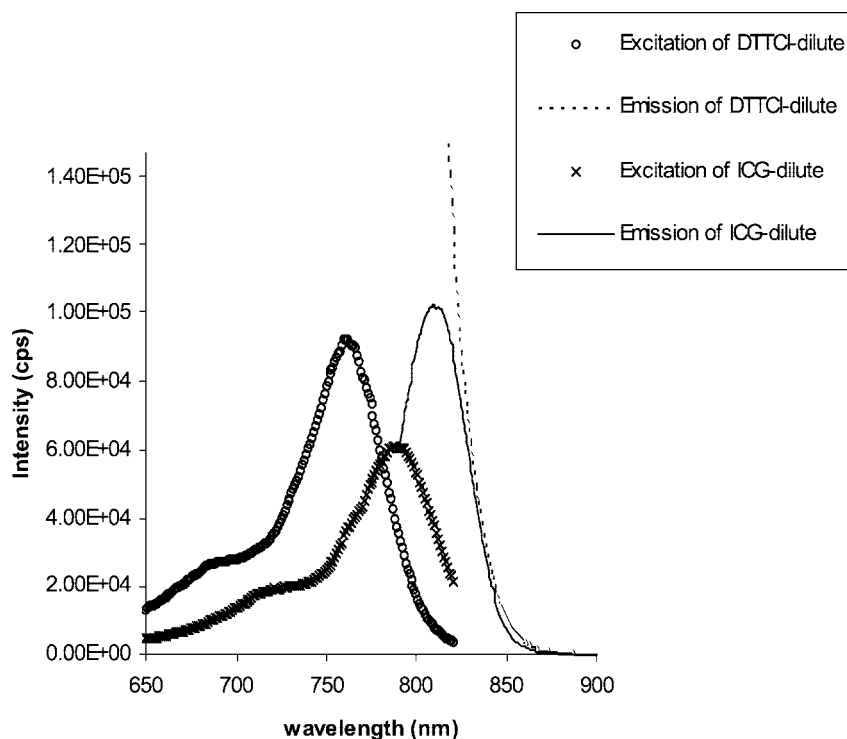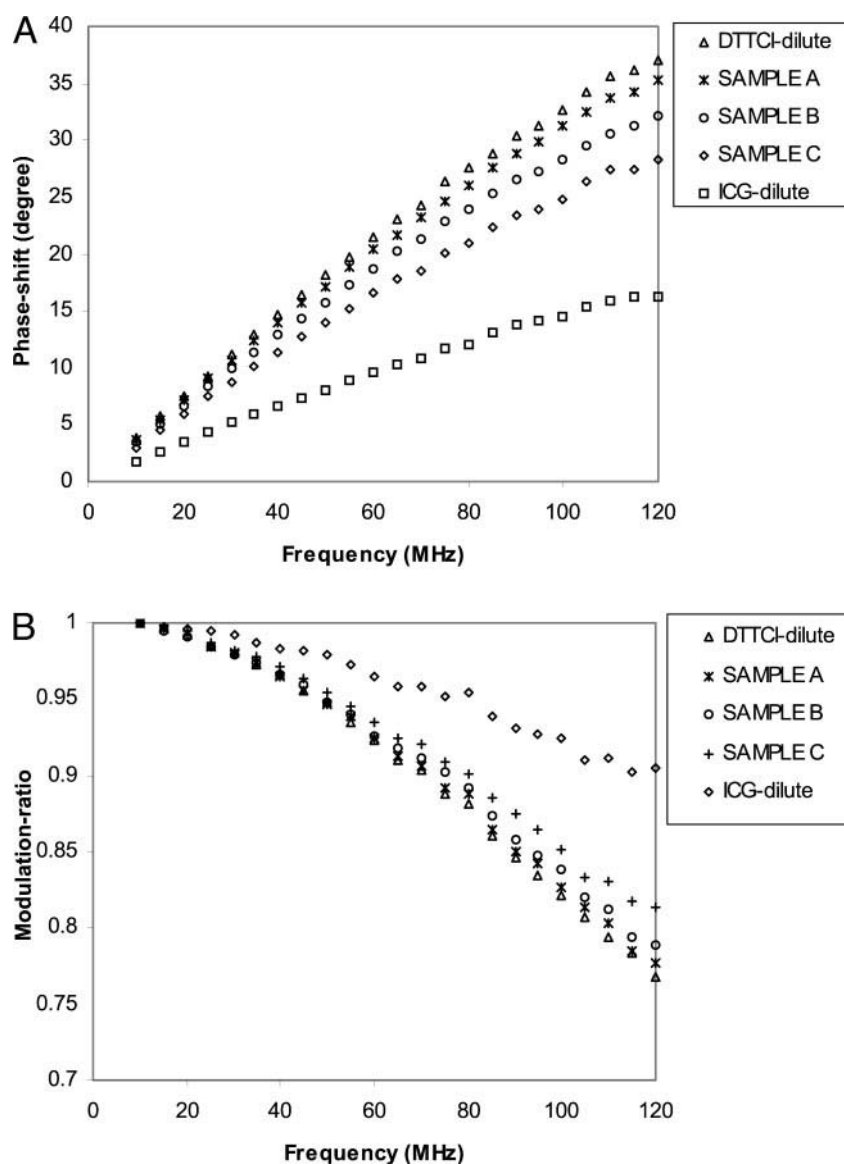
FIGURE 4 Corrected values of fluorescence phase-shift (*A*) and modulation-ratio (*B*) versus modulation frequency for pure DTTCI (DTTCI-dilute), pure ICG (ICG-dilute), as well as for ICG-DTTCI solution mixture at various concentration ratios in nonscattering solution (50% EtOH). Samples were excited at 778 nm, and the emission was observed at 830 nm.

were found to be as much as 3% and 1% from the true values for ICG and DTTCI lifetime. When 5% error was considered, the optimization failed to produce results from low frequency phase-modulation data limited to 120 MHz. Hence, phase-modulation values measured at high frequencies in nonscattering solution are crucial for successful recovery of lifetime, especially for subnanosecond decay kinetics. In conclusion, the results presented in Table 2a may be consistent with independent relaxation kinetics for the two dyes as modeled by an average and biexponential decay model.

However, if the decay kinetics of ICG and DTTCI are not independent and quenching occurs, then the stretched exponential decay functions may be used to describe the decay kinetics. Originally, the multiexponential model was used as an approximation to the stretched exponential decay kinetics (Hirayama et al., 1990), whereby an infinite number of

components could provide adequate representation. Because of the complexities associated with deconvolution procedures, particularly for those working in time-domain, recent studies in fluorescence lifetime tend to use multiexponential rather than stretched exponential models. Many even further simplify multiexponential into global multiexponential model in which τ_j in Eq. 1 are assumed to be constants. In this study, we investigated stretched exponential decay kinetics to find a justifiable model, especially as the simple two component multiexponential function fails in presence of scattering (see below) and as the presence of scattering increases the range of phase and amplitude measurements, which consequently enhances the sensitivity to intrinsic kinetics.

The multiexponential decay parameters a_j and $\tau_j(j = 1, n)$ were then used to generate a decay profile from Eq. 1 and then fitted to the kinetic models of 1) stretched exponential

TABLE 2 Decay analysis at various mixture ICG-DTTCI concentrations in nonscattering 50%-EtOH solutions based on (*a*) biexponential, (*b*) stretched exponential, and (*c*) bistretched exponential models

Samples	a_1	f_1	τ_1 (ns)	a_2	f_2	τ_2 (ns)	τ_{avg} (ns)
I-D_0.05–0.5	0.59	0.32	0.43	0.41	0.68	1.32	1.03
I-D_0.15–0.5	0.77	0.50	0.43	0.23	0.50	1.47	0.95
I-D_0.4–0.5	0.84	0.58	0.39	0.16	0.42	1.51	0.86

Samples	a_1	α (1/ns)	β (1/ns^0.5)	a_2	τ_2 (ns)
I-D_0.05–0.5	0.59	1.04	2.88	0.41	1.32
I-D_0.15–0.5	0.77	1.19	3.16	0.23	1.47
I-D_0.4–0.5	0.84	2.00	2.06	0.16	1.51

Samples	a_1	α_1 (1/ns)	β_1 (1/ns^0.5)	a_2	α_2 (1/ns)	β_2 (1/ns^0.5)
I-D_0.05–0.5	0.55	1.38	4.21	0.45	0.75	0.07
I-D_0.15–0.5	0.70	1.42	3.39	0.30	0.65	0.20
I-D_0.4–0.5	0.84	1.72	6.54	0.16	0.66	0.00

Samples were excited at 778 nm and the emission was observed at 830 nm. Species 1 and 2 corresponds to ICG and DTTCI, respectively.

with a single exponential decay component (Table 2b) as well as 2) bistretched exponential decay (Table 2c). We fit the scattering data to the maximal number of exponential terms, which did not result in an increase in sum of square errors. In our case, the maximum number of exponential terms required to provide the best fit was $n = 3$. In the model using stretched exponential decay kinetics, ICG presumably acts as a quencher to DTTCI as indicated by the lifetime of the single exponential decay component of the model. To explore the possibility that the two dyes are mutually quenched, the bistretched exponential model was fit to the scattering data. It is noteworthy that the results for the bistretched exponential decay kinetics model also indicates that ICG does not act as the donor as the parameter estimate of β associated with the inverse lifetime (or α) corresponding to ICG is zero.

In conclusion, the results from measurements in nonscattering solutions show the inability to completely discriminate decay kinetic models at moderate modulation frequencies (10–120 MHz) for the two dyes with lifetimes separated by a factor of 2.

Fluorescence multiexponential decay in scattering media

The variations of ICG-DTTCI concentration ratio investigated in scattering measurements were similar to that in the nonscattering measurements. Each 500-mL sample contained 2% (volume) of intralipid in a water-EtOH mixture (1:1 volumetric ratio) solvent (Table I). The multiplexed fluorescence phase-shift and modulation-ratio data were substituted into Eqs. B5 and Eq. B6 (see Appendix B), and the corrected values of θ and M are plotted in Fig. 5. Comparison of Figs. 4 and 5 shows that scattering contrib-

utes significantly to the phase-shift and modulation-ratio values.

Model predictions of multiexponential lifetime decay in scattering

If the optical properties and decay kinetics information of a scattering sample containing a fluorescence dye are known, the phase-shift θ_f and modulation-ratio M_f due to the fluorophore lifetime and the fluorescence light propagation can be predicted. In this study, θ_f and M_f are modeled as the phase shift and modulation ratio arising from the propagation of excitation and the generated emission light and from the independent relaxation of the two dyes, or the quenching of one or both of the dyes. In the first case, the intrinsic kinetic models incorporated into the diffusion model were 1) biexponential decays and 2) the weighted average of the biexponential decay. In the second case, the intrinsic models used within the diffusion model were either 1) a stretched exponential function to describe the donor fluorescence and a single exponential decay component or (2) bistretched exponential decay kinetics to describe mutual quenching between the two dyes. For the case that the decay kinetics are described by the stretched exponential decay, numerical integration was performed in mathematica. Problems such as cut-off effects were not encountered in the range of frequency such as that obtained in the data acquisition owing to the sharp decay of the stretched exponential functions (short lifetime).

The optical properties of the scattering samples at various ICG-DTTCI concentrations are shown in Table III. The values were obtained from emission and excitation measurements and from Eq. C1 (see Appendix C), in which K_{DC} and K_θ were the slopes obtained by linear regression (Sun et
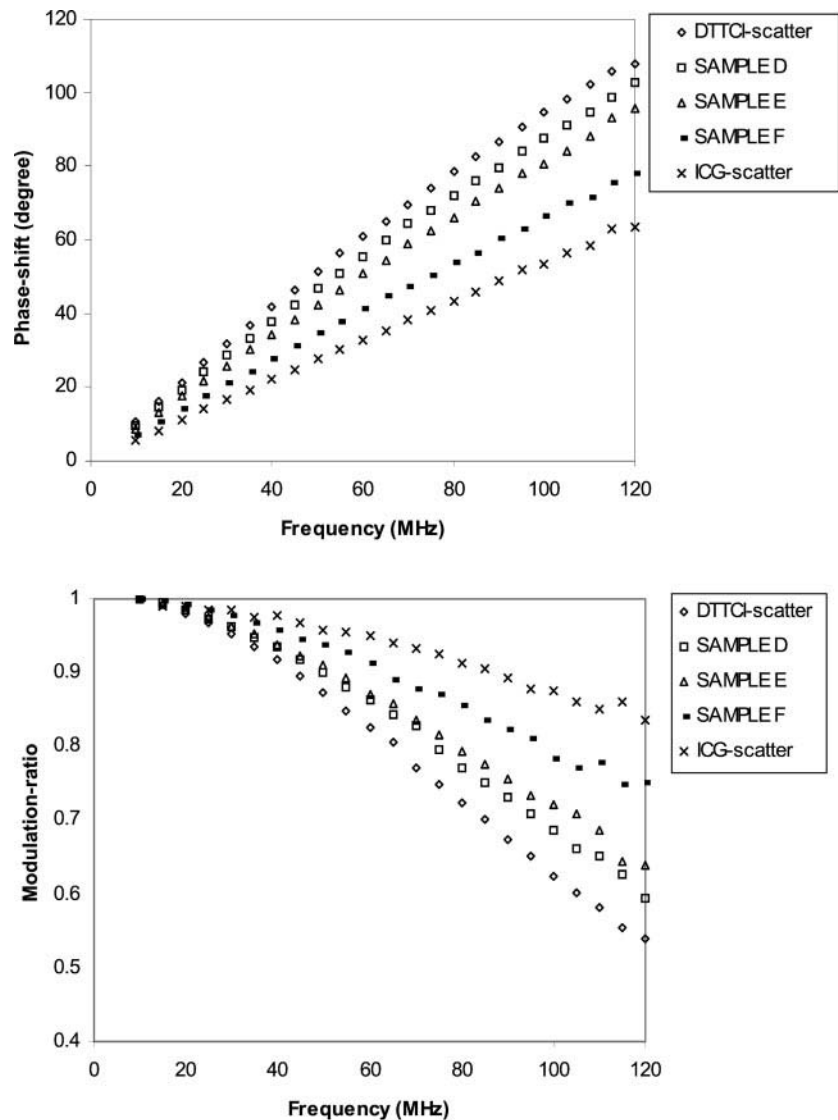
FIGURE 5 Corrected values of fluorescence phase-shift (*a*) and modulation-ratio (*b*) versus modulation frequency for pure DTTCI (DTTCI-scatter), pure ICG (ICG-scatter), as well as for ICG-DTTCI mixture at various concentration ratios in scattering solution (2% intralipid). Samples were excited at 778 nm, and the emission was observed at 830 nm. The distances r_1 and r_2 in Fig. 2 *b* were 1 cm and 1.8 cm, respectively.

al., 2002) at a fixed modulation frequency and varying source-detector separation ($r_2 - r_o$) in Fig. 2 *B*. The values of $\mu_{a,x}$ increase with dye concentrations was as expected.

TABLE 3 Optical properties of scattering samples at various ICG-DTTCI concentration ratios

Samples	$\mu_{a,x}$ (1/cm)	$\mu_{a,m}$ (1/cm)	$\mu'_{s,x}$ (1/cm)	$\mu'_{s,m}$ (1/cm)
DTTCI-scatter	0.11	0.03	15.77	14.60
SAMPLE D	0.17	0.03	15.07	13.29
SAMPLE E	0.18	0.03	15.24	12.33
SAMPLE F	0.31	0.06	15.18	10.86
ICG-scatter	0.21	0.03	12.90	10.05

Results were obtained by linear regression of θ and M as a function of ($r_2 - r_o$) where the modulation frequency was fixed at 100 MHz and ($r_2 - r_o$) in Fig. 2 *b* were varied between 1.5 and 2 cm. The subscripts x and m signify laser source at excitation (778 nm) and emission (828 nm) wavelengths, respectively.

The slight variation of $\mu_{a,m}$, $\mu_{s,x}$, and $\mu_{s,m}$ values at different concentration ratios may be due to the error associated with the regression.

Fig. 6 shows the dependence of fluorescence phase shift and modulation ratio upon modulation frequency for SAMPLE E in 2% intralipid solution as measured experimentally and predicted by the solution to the diffusion equation that incorporated the four different kinetic models, 1) biexponential decay, 2) single exponential decay representing average lifetime of the bi-exponential decays, 3) stretched exponential decay with a single exponential decay component, and finally 4) bistretched exponential decay models. Specifically, we used the parameter estimates of the four kinetic models obtained from measurements in nonscattering solutions and presented in Table 2. Although all four intrinsic kinetic models provided comparable fit with values of θ_f and M_f measured in nonscattering solution, in the
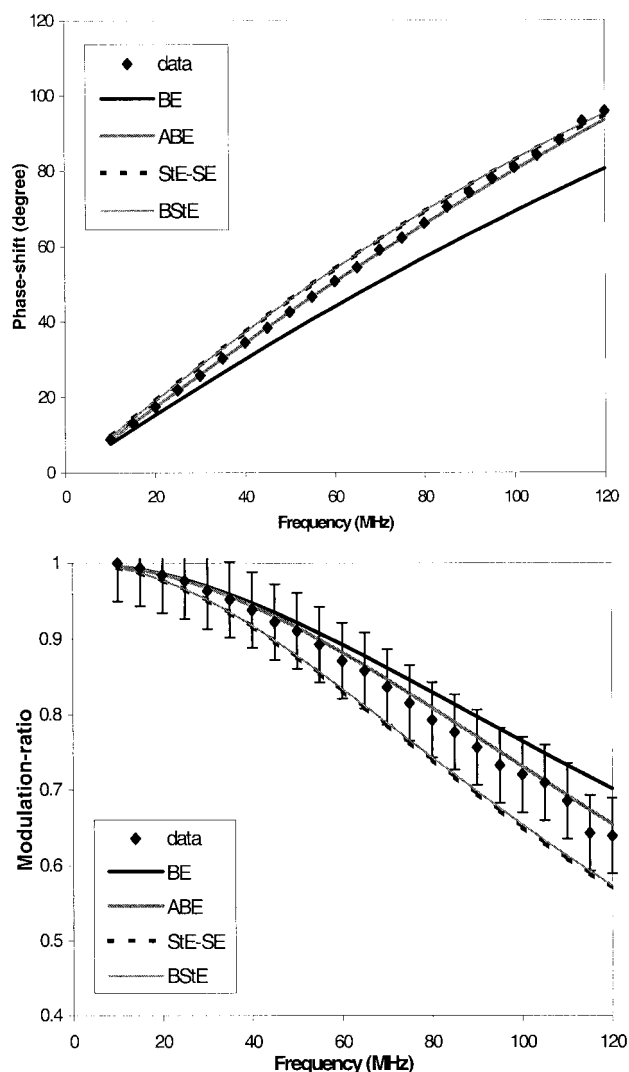
TABLE 4 Average lifetime values calculated from phase-shift data in presence of scattering, assuming multiexponential decay kinetics at a fixed frequency of 80 MHz

Samples	$\langle \tau \rangle$ (ns)
SAMPLE D	1.02
SAMPLE E	0.96
SAMPLE F	0.88

the four decay models. The bistretched exponential model and the stretched exponential model incorporating a single decay component provide identical results that predict well the phase-shift data but less accurately predict modulation data. On the other hand, the biexponential decay model fails to predict either the phase-shift or modulation data suggesting that independent relaxation of the two dyes does not occur. However, the single decay model that incorporates an average lifetime provides the best match to both the phase-shift and the modulation data. Similar results are obtained from the remaining samples with differing fluorophore concentration ratios.

Whereas the nonscattering data provided no discrimination between the intrinsic kinetic models, the measurement data made in the presence of scattering and predicted by the diffusion equation show that the intrinsic kinetic models may very well be discriminated from one another. Yet, owing to the difficulty in extracting decay kinetics directly from the measurement data made in the presence of scattering, our results cannot be used to definitively determine which decay model fits the scattering data best. Whereas the lack of agreement with the biexponential model prediction indicates the relaxation processes of the two dyes are indeed dependent, the stretched exponential and bistretched exponential models more closely predict the phase data obtained in the presence of scattering. Most curiously, the average or single exponential decay model fits best.

Fig. 6 also shows that in all of the decay models evaluated, the values of modulation ratio are not well predicted. One reason for the lack of fitting may be the difficulty in obtaining precise modulation data, especially in absence of scattering, that critically depends on the stability of source intensity, consistency of detection apparatus, presence of ambient light, or electrical disturbances, etc.

Due to the fact that the fluorescence data measured in presence of scattering are in good agreement with the average lifetime model, fluorescence lifetime sensing of dyes exhibiting multiple decays may be performed by simply obtaining the average lifetime. Table 4 shows the average lifetime values $\langle \tau \rangle$ that was recovered from phase-shift data acquired in presence of scattering, at a fixed frequency of 80 MHz. The values in Table 4 are in good agreement with τ_{avg} shown in Table 2a. In absence of scattering, subnanosecond lifetime detection would be difficult at such low modulation frequency (as discussed

FIGURE 6   Values of fluorescence phase-shift (*a*) and modulation-ratio (*b*) as a function of modulation frequency for corrected experimental measurements on SAMPLE E (*black diamond*), and that predicted by the propagation model incorporating biexponential decay kinetics (BE) (*bold black line*), average bi-exponential decay (ABE) (*bold gray line*), the stretched exponential decay with a single exponential decay component (StE-SE) (*dotted black line*), and the bistretched exponential decay (BStE) (*thin gray line*). Values from Table 2 provide the parameter for predictions. The refractive index of the medium was assumed to be that of 50%-EtOH (1.345).

presence of scattering, the intrinsic kinetic models incorporated into the diffusion equation could not provide comparable fits. Our results show that the values of θ_f and M_f predicted from the diffusion equation incorporating the four exponential models exhibit the same trend as that exhibited by the experimental data for the various concentration ratios of the two dyes as illustrated in Fig. 5.

Fig. 6 illustrates the experimental values of phase shift and modulation ratio measured from SAMPLE E and those that are predicted from the diffusion equation incorporating

in the optimization study). The presence of scattering however, magnifies the measured phase-shift value, and hence increases the sensitivity of lifetime sensing, given that the optical properties of the scattering solution can be accurately predicted.

CONCLUSIONS

In this contribution, we have extended fluorescence lifetime spectroscopy in scattering solution to fluorophores that exhibit intrinsic decays not attributed to first order kinetics. Specifically, we used the diffusion equation to describe the propagation of excitation and emission light in scattering media and incorporated the intrinsic decay kinetics described by average, multi-, and stretched-exponential decay models to predict frequency-domain measurements of multiply scattered emission light and demonstrate fluorescence spectroscopy in scattering solution.

The fluorescence decay kinetics of two emitting dyes in nonscattering solutions could be equally well predicted by 1) biexponential decay, 2) a stretched exponential with a single exponential component, and 3) a bistretched exponential decay model. However, when the parameter estimates from those models were used to predict frequency-domain measurements in scattering solutions using the optical diffusion equation, there was little agreement in the moderate frequency range used. Yet the average lifetime obtained from the parameter estimates in the biexponential model fit the data obtained in the scattering solutions comparably better.

These results suggest that frequency-domain measurements of fluorescent decay kinetics may be augmented with scatter to probe kinetics more sensitively than in nonscattering solutions. Future work involves assessing the multiple scattered data to directly obtain parameters estimates of the kinetic models, as done with τ_{avg} in the current study.

APPENDIX

Correction for instrument function of fluorescence measurements in nonscattering media

The measured relative phase shift θ_{rel} consists of both the phase-lag θ due to the lifetime of the fluorophore in the sample and the instrument response function θ_{instr}. Similarly, the measured relative modulation M_{rel} consists of both the modulation-ratio M due to the lifetime of the fluorophore and the instrument response function M_{instr}.

$$\theta_{rel} = \theta + \theta_{instr} \tag{A1}$$

$$M_{rel} = M M_{instr} \tag{A2}$$

A reference dye of known lifetime can be used to correct these instrument functions. The reference dye is excited at the same excitation wavelength as the dye of interest. Also, the detected fluorescence light of the reference dye is the same as the fluorescence wavelength of the dye of interest. The measured relative phase shift and modulation of the reference dye (θ_{rel}^{ref} and M_{rel}^{ref}) are given by

$$\theta_{rel}^{ref} = \theta^{ref} + \theta_{instr} \tag{A3}$$

$$M_{rel}^{ref} = M^{ref} M_{instr} \tag{A4}$$

in which θ^{ref} and M^{ref} can be calculated at various modulation frequency assuming the reference dye exhibit single exponential decay (hence, $\theta = \arctan(\omega\tau)$ and $M^{-1} = (1 + (\omega\tau)^2)^{0.5}$).

Combining Eq. A1 and A3 to get the expression for phase-shift and Eq. A2 and A4 for the modulation resulting from the dye of interest

$$\theta = (\theta_{rel} - \theta_{rel}^{ref}) + \theta_{ref} \tag{A5}$$

$$M = \left(\frac{M_{rel}}{M_{rel}^{ref}}\right) M^{ref} \tag{A6}$$

Correction for instrument function of fluorescence measurement in scattering media

The instrument response function for the FDPM measurements in scattering media can be corrected without the use of reference dye. The correction can be obtained by multiplexing the optical signals of the two detector fibers at two different positions in the sample (Mayer et al., 1999). The two detector fibers shown in Fig. 2 B are of the same length, to ensure equal optical path lengths of the two signals.

The measured relative phase shift and modulation reflects light propagation (and fluorescence generation, in the case of fluorescence measurements) in the sample as well as the instrument function

$$\theta_{rel,12} = \theta + \theta_{instr} \tag{B1}$$

$$M_{rel,12} = M M_{instr} \tag{B2}$$

After multiplexing:

$$\theta_{rel,21} = -\theta + \theta_{instr} \tag{B3}$$

$$M_{rel,21} = \frac{1}{M} M_{instr} \tag{B4}$$

in which the subscript 12 denotes the relative value of the signal detected by PMT_1 to the signal detected by PMT_2, and the subscript 21 denotes the otherwise.

Combining Eqs. B1 and B3 and Eqs. B2 and B4, one can obtain the phase shift and modulation ratio that are devoid of instrument function:

$$\theta = \frac{1}{2} (\theta_{rel,12} - \theta_{ref,21}) \tag{B5}$$

$$M = \left(\frac{M_{rel,12}}{M_{rel,21}}\right)^{1/2} \tag{B6}$$

For the case of fluorescence photon density measurements, the instrument function may not be completely corrected by multiplexing method because signals obtained at the two detectors in fluorescence measurement are of different wavelengths, and photocathode response is wavelength dependent. However, we found this uncorrected error to be negligible after subsequent multiplexing (Mayer et al., 1999).

Correction for excitation and emission measurements in scattering media

Theoretically, the multiplexing method described in previous section can be performed for excitation and emission measurements as well, and hence single distance (multifrequency) nonlinear regression (Fishkin et al., 1995) can be performed to obtain optical properties of the medium. But a recent study in our laboratory showed that measurements made at multidistances enable linear regression of parameters (Fishkin et al., 1995) and results in the most precise optical property information (Sun et al., 2002).

In this study, using the relative I_{dc} and θ information measured between the two fibers in Fig. 2 *b*, one can obtain the optical properties of the medium, μ_a and μ_s, by the following relationships (Sun et al., 2002):

$$\mu_a = \frac{\omega}{\nu}\left\{[2(K_\theta/K_{DC})^2 + 1]^2 - 1\right\}^{-1/2} \qquad \mu_s' = \frac{K_{DC}^2}{3\mu_a} - \mu_a$$

$$(C1)$$

in which K_{DC} and K_θ are slopes of the straight lines obtained from linear regression of the relative I_{dc} and θ data at varying distances between the two fibers for a given modulation frequency.

REFERENCES

Andersson-Engels, S., J. Johansson, K. Svanberg, and S. Svanberg. 1991. Fluorescence imaging and point measurements of tissue: applications to the demarcation of malignant-tumors and atherosclerotic lesions from normal tissue. *Photochem. Photobiol.* 53:807–814.

Cerussi, A. E., S. Fantini, M. A. Franceschini, E. Gratton, J. S. Maier, and W. W. Mantulin. 1997. Experimental verification of a theory for the time-resolved fluorescence spectroscopy of thick tissues. *Appl. Optics.* 36:116–124.

Fishkin, J. B., A. E. Cerussi, S. Fantini, M. A. Franceschini, E. Gratton, and P. T. C. So. 1995. Frequency-domain method for measuring spectral properties in multiple scattering media: methemoglobin absorption spectrum in a tissue-like phantom. *Appl. Opt.* 34:1143.

Fishkin, J. B., and E. Gratton. 1993. Propagation of photon-density waves in strongly scattering media containing an absorbing semiinfinite plane bounded by a straight edge. *J. Opt. Soc. Am. A.* 10:127–140.

Gratton, E., H. Cherek, G. Laczko, J. R. Lakowicz, M. Limkeman, and B. P. Maliwal. 1984. Resolution of mixtures of fluorophores using variable-frequency phase and modulation data. *Biophys. J.* 46:479–486.

Hawrysz, D. J., and E. Sevick-Muraca. 2000. Development toward diagnostic breast cancer imaging using near-infrared optical measurements and fluorescent contrast agents. *Neoplasia.* 2:338–417.

Hirayama, S., K. P. Ghiggino, Y. Sakai, and T. A. Smith. 1990. The application of a simple deconvolution method to the analysis of stretched-exponential fluorescence decay functions. *J. Photochem. Photobiol. A.* 52:27–38.

Hutchinson, C. L., T. L. Troy, and E. M. Sevick-Muraca. 1996. Fluorescence-lifetime determination in tissues or other scattering media from measurement of excitation and emission kinetics. *Appl. Optics.* 35: 2325–2332.

Inokuti, M., and F. Hirayama. 1965. Influence of energy transfer by the exchange mechanism on donor luminescence. *J. Chem. Phys.* 43: 1978–1989.

James, D. R., and W. R. Ware. 1985. A fallacy in the interpretation of fluorescence decay parameters. *Chem. Phys. Lett.* 120:455–459.

Lakowicz, J. R. 1983. Principles of Fluorescence Spectroscopy, 1st Ed. Plenum Press, New York.

Lakowicz, J. R., and O. O. Abugo. 1999. Modulation sensing of fluorophores in tissue: a new approach to drug compliance monitoring. *J. Biomed. Opt.* 4:429–442.

Lakowicz, J. R., H. Cherek, E. Gratton, G. Laczko, and M. Limkeman. 1984. Analysis of fluorescence decay kinetics from variable-frequency phase-shift and modulation data. *Biophys. J.* 46:463–477.

Lakowicz, J. R., and H. Szmacinski. 1992. Calcium imaging using fluorescence lifetimes and long-wavelength probes. *J. Fluoresc.* 2:47–62.

Lakowicz, J. R., and H. Szmacinski. 1993. Optical measurements of pH using fluorescence lifetimes and phase-modulation fluorometry. *Anal. Chem.* 65:1668–1674.

Mayer, R. H., J. S. Reynolds, and E. Sevick-Muraca. 1999. Measurement of the fluorescence lifetime in scattering media lay frequency-domain photon migration. *Appl. Optics.* 38:4930–4938.

Nemzek, T. L., and W. R. Ware. 1975. Kinetics of diffusion-controlled reactions: transient effects in fluorescence quenching. *J. Chem. Phys.* 62:477–489.

Press, W. H., B. P. Flannery, S. A. Teukolsky, and W. T. Vetterling. 1992. Numerical Recipes in Fortran—The Art of Scientific Computing, 2nd Ed. University Press, Cambridge.

Qing, C., J. R. Lakowicz, Z. Murtaza, and G. Rao. 1997. A fluorescence lifetime-based solid sensor for water. *Anal. Chim. Acta.* 350:97–104.

Russell, R. J., G. L. Cote, C. C. Gefrides, M. J. McShane, and M. V. Pishko. 1999. A fluorescence-based glucose biosensor using concanavalin A and dextran encapsulated in a poly(ethylene glycol) hydrogel. *Anal. Chem.* 71:3126–3132.

Sevick, E. M., B. Chance, J. Leigh, M. Maris, and S. Nioka. 1991. Quantitation of time-resolved and frequency-resolved optical-spectra for the determination of tissue oxygenation. *Anal. Biochem.* 195:330–351.

Sun, Z., Y. Huang, and E. M. Sevick-Muraca. 2002. Precise analysis of frequency-domain photon migration measurement for characterization of concentrated colloidal suspensions. *Rev. Sci. Instrum.* 73:383–393.

Weissleder, R., A. Bogdanov, U. Mahmood, and C. H. Tung. 1999. In vivo imaging of tumors with protease-activated near-infrared fluorescent probes. *Nat. Biotech.* 17:375–378.